OPTIMUM STRUCTURAL DESIGN OF CFRP ISOGRID CYLINDRICAL SHELLS

G. BEN[1*], T.SUZUKI[2] , K.SAKATA[1]

[1]*College of Industrial Technology, Nihon University, 1-2-1, Izumicho, Narashino, Japan.*
[2]*Graduate Student of Nihon University, 1-2-1, Izumicho, Narashino, Japan.*
**e-mail address: ben.goichi@nihon-u.ac.jp*

Keywords: Isogrid shell, CFRP, Optimum design, GA, RSM

Abstract
With a good agreement between buckling analyses by FEM and uniaxial compression tests for the CFRP isogrid cylindrical shells, this paper describes an optimum design of CFRP isogrid cylindrical shell. When the CFRP isogrid cylindrical shell receives a prescribed uniaxial compressive load, the object is to minimize the weight of the CFRP isogrid cylindrical shell subjected to constraint conditions of no failure and no buckling by using the genetic algorithm (GA) method. In the GA process, the buckling and CFRP failure loads were obtained by an approximated function formulated with the moving least square (MLS) method for saving computational resources.

1. Introduction

Isogrid stiffened cylindrical shells are composed of a surface skin shell and repetitive equilateral triangular grid stiffeners and they demonstrate a higher specific strength and stiffness due to their lightweight. An integral molding method of CFRP isogrid cylindrical shells was developed by using a filament winding apparatus [1] and a revised method with a silicone rubber mold [2]. A. D. Reddy [3] studied the buckling response of isogrid cylindrical shells with various stiffener spacing using global and local analyses. A literature survey on the optimal design of stiffened panels and shells was presented in [4]. N. Jaunky et al [5] presented the analysis and weight optimization strategy for grid stiffened composite circular cylindrical shells using the genetic algorithm. D.R.Ambur [6] showed the optimal design of grid stiffened panels and shells with variable curvature. Furthermore, G.Totaro [7] dealt with optimization of composite lattice shells structures (without skin).

This paper describes numerical analyses for the CFRP isogrid cylindrical shells under a uniaxial compression. In the numerical method using the finite element code of ANSYS, an eigen-value analysis for obtaining a linear buckling load and a nonlinear incremental displacement method for obtaining local and global buckling loads were carried out. The experimental results showed a reinforcement effect of isogrid stiffeners on the CFRP cylindrical shell and they agreed well with those obtained from the numerical analyses. Furthermore, an optimum problem was demonstrated, namely three design parameters, such as the winding angle of skin cylindrical shell and the width and the number of lamination (thickness) in the isogrid stiffeners were selected among many design parameters. The object was to minimize the weight of the CFRP isogrid cylindrical shell with the constraint conditions of no failure and no buckling under the prescribed uniaxial compression load.

2. Experiments

The surface skins in a CFRP isogrid cylindrical shell having winding angles of 90 degrees (Iso-90) or ±60 degrees (Iso-60) were fabricated with the CFRP tow prepreg (TR50S, MITSHBISHI RAYON CO.) and an FW machine. The same CFRP cylindrical shell without grid stiffeners (Non-90 and Non-60) and a grid shell without the surface skin (Grid) were also fabricated. The number of specimens was three for each of the shell types.

Table 1 lists the average sizes of the five shell types. In Table 2, the maximum compressive loads obtained by the experiment and their average are listed. In the experimental results, there were small deviations among the three specimens for the five shell types. The experimental maximum compressive load of the Iso-90 was 2.6 times higher than that of the Non-90 and this value was larger than the sum of the maximum values of the Non-90 and of the shell of grid alone. The experimental maximum compressive load of the Iso-60 was 2.2 times higher than that of the Non-60 and this value was also larger than the Non-60 and the shell of grid alone. These facts showed the reinforcement effect on the CFRP cylindrical shells with the isogrid stiffeners.

Type of test specimen	CFRP Isogrid cylindrical shell		CFRP monocoque cylinder		Shell of Isogrid alone
Lable	Iso-90	Iso-60	Non-90	Non-60	Grid
Winding angle of skin	90	60	90	60	—
Shell length [mm]	137.5	135.1	139.0	138.4	137.8
Inner diameter [mm]	108.5	110.8	110.0	110.4	106.3
Plate thickness [mm]	0.8	0.6	0.9	0.7	—
Stiffener width [mm]	2.0	2.2	—	—	2.3
Stiffener height [mm]	2.5	3.2	—	—	2.0

Table 1 Average dimension of 5 kinds of test shells

	Maximum Load [kN]				
	Non-90	Non-60	Grid	Iso-90	Iso-60
No.1	14.2	14.8	9.8	36.3	31.8
No.2	13.9	12.8	9.3	39.6	29.0
No.3	15.4	14.2	9.5	37.5	31.5
Ave	14.5	13.9	9.5	37.8	30.7

Table 2 Compressive Maximum Load in Experiments

3. Numerical Analyses

The numerical analysis was performed with a finite element code in ANSYS Version11.0 and the 4 node layered structural element (code name:SHELL181) was used for modeling the surface skin of the cylindrical shell and the grid stiffeners and then common nodes were used between the surface and the grids. Since the CFRP isogrid cylindrical shells exhibited cyclic symmetry (a single of 45º sector) and their boundary condition had repetitive patterns, we used the ANSYS-automated cyclic symmetry analysis. The cyclic symmetry model (basic sector) is shown in Figure 1. The boundary conditions of the cyclic symmetry model at both of the axial ends were assumed to be simply supported. The number of nodes and elements of

the FEM model were 5,531 and 5,064, respectively. The material constants and strength of CFRP used in the FEM analysis are listed in Tables 3 and 4.

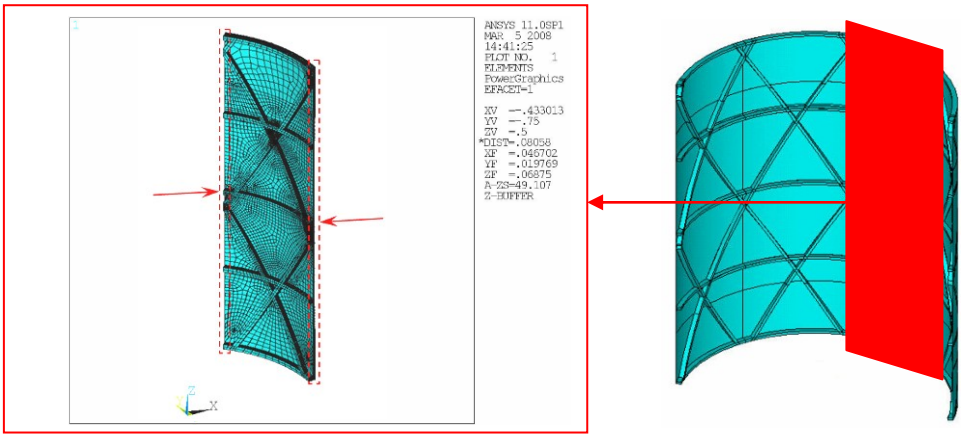

Figure 1 CFRP isogrid cylindrical shell model and repetitive model

		Tensile	Compressive
Longitudinal Modulus [GPa]	E_X	142	129
Transverse Modulus [GPa]	E_Y	8.8	9.3
	E_Z	8.8	9.3
Shear Modulus [GPa]	G_{XY}	4.2	
	G_{YZ}	3.3	
	G_{XZ}	4.2	
Poisson's Ratio	ν_{XY}	0.32	
	ν_{YZ}	0.40	
	ν_{XZ}	0.32	

		Tensile	Compressive
Longitudinal Strength [MPa]	F_X	2950	1570
Transverse Strength [MPa]	F_Y	79	190
Shear Strength [MPa]	F_{XY}	140	

An eigen-value calculation for obtaining the linear buckling loads and a nonlinear iterative calculation for the local buckling (the surface skin buckling) and the global buckling load were separately carried out. In the nonlinear calculation, an axial symmetric deformation in the pre-buckling state was used but initial imperfection modes were not considered. Furthermore the Tsai-Wu criterion was used to judge the failure of CFRP isogrid cylindrical shells in the process of the nonlinear calculation. This failure load was compared with the local buckling load which was obtained by the P-δ^2 method. Figure 2 shows the relationship of the compressive load to the axial displacement for the Iso-90. The curve showed considerable nonlinearity after the local buckling and its global buckling loads were almost

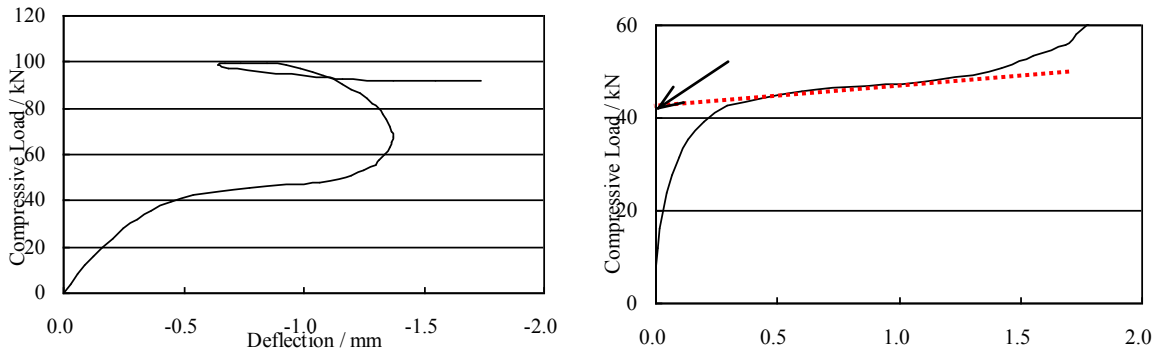

100 kN. Figure 3 shows the local buckling loads obtained by the P-δ^2 method and it was 42.0 kN. In the Iso-60, the local buckling load was obtained as 32.0 kN by the same method.

4. Comparison of experiment with analysis

The average values of the experimental maximum load for the five specimens are listed in Table 5 and they were compared with the buckling loads calculated from the analytical formula [4] and the linear buckling loads obtained by the eigen-value analysis, the local buckling loads, the global buckling loads obtained by the nonlinear analysis and the failure loads based on the Tsai-Wu criterion.

The analytical asymmetric buckling loads for the Non-90 and the Non-60 were close to the linear buckling load but they were larger than those of the experiment. However, the nonlinear (local) buckling loads were closer to those of the experiment.

Since the local buckling load was larger than the failure load in the comparison of the Iso-90, the Iso-90 seemed to be the material failure, not the buckling failure. On the other hand, the local buckling load of the Iso-60 was smaller than the failure load and it was closer to the experimental result than that of failure. So, the Iso-60 seemed to be the buckling failure.

	Experimental Value [kN]	Analytical Formula		FEM Analysis			
		Symmetry [kN]	Asymmetry [kN]	Linear Buckling Load [kN]	Local Buckling Load [kN]	Global Buckling Load [kN]	Failure Load [kN]
Non-90	14.5	35.5	18.1	18.3	—	14.4	36.3
Non-60	13.9	34.4	33.4	33.6	—	28.0	63.3
Grid	9.5	—	—	18.2	—	16.5	—
Iso-90	37.8	—	—	80.6	42.0	100.0	40.2
Iso-60	30.7	—	—	71.5	32.0	100.5	38.2

Table 5 Comparisons of experimental results with FEM

5. Optimum design

Although the number of skin layers and their winding angles could be considered as the design parameters, the only one couple of angle ply layers (its angle) was treated as the design parameter x1 in order to focus on the effects of the isogrid stiffeners. The widths and the number of layers (thickness) of isogrid stiffeners in the helical and circumferential directions were all the same and they were treated as the design parameters of x2 and x3. On the other hand, the winding angle of stiffeners in the helical direction was a constant of 30 degrees because the isogrid shape was kept. The radius and length of isogrid cylindrical shell were constant of 55 mm and 150 mm. The offset of isogrid surrounded with the circumferential stiffener and the helical stiffeners was a constant value of 3mm because the effect of offset size on the buckling load was comparatively smaller than those of other design parameters. Although the numbers of circumferential stiffeners should be treated as the design parameters, the optimum calculation was here executed under the constant values of 3.

5.1 Object Function and Constraint Condition

The object was to minimize the weight of isogrid CFRP cylindrical shell under the compressive load Ps (prescribed value) which was smaller than the buckling load and the CFRP failure loads. In this case, the CFRP failure load was defined as the larger value than 1 in the Tsai-Wu criterion and the optimum problem was summarized in Equation (1)

Find : Design parameters x=[x1,x2,x3] subjected to Ps<Pb (Buckling Load)[N]
Minimize : W(weight) [N] Ps<Pm (Failure load) [N]
22<x1<90 [deg]
2.0<x2<6.0 [mm]
1<x3<32 [ply] (1)

100 sets of design parameters were selected randomly from the design space and the final 100 data sets were determined by the Mitchell exchange method in the D-optimal. Then the resulting buckling loads and CFRP failure loads under the prescribed load were calculated for these data sets by the FEM.
Since the buckling and CFRP failure loads should be calculated many times in the optimum process, it is better to use approximate functions for obtaining both loads instead of the FEM for saving the computational hours. Since both loads seemed to have the multiple local maxima for the change of design parameters, the following equations for approximating the buckling and CFRP failure loads were separately formulated by the MLA (moving least-square approximation) in order to increase the accuracy of approximation.

$$y(x) = a_0 + a_1x_1 + a_2x_2 + a_3x_3 + a_4{x_1}^2 + a_5{x_2}^2 + a_6{x_3}^2 + a_7x_1x_2 + a_8x_1x_3 + a_9x_2x_3$$
$$= p(x)^T a(x) = p(x)^T \mathrm{A}^{-1}(x)B(x)u \quad (2)$$

$$\begin{cases} p(x_i) = \left\{1, x_{i1}, x_{2,i}, x_{3,i}, {x_{1,i}}^2, {x_{2,i}}^2, {x_{3,i}}^2, x_{1,i}x_{2,i}, x_{1,i}x_{3,i}, x_{2,i}x_{3,i}\right\}^T \\ \mathrm{A}(x) = \sum_{i=1}^{N} w(r_i)p(x_i)p(x_i)^T \\ B(x) = \left\{w(r_1)p(x_1), w(r_2)p(x_2), \cdots, w(r_N)p(x_N)\right\} \\ w(r_i) = 1 - 6(r_i/\rho)^2 + 8(r_i/\rho)^3 - 3(r_i/\rho)^4 \\ u = \left\{u_1, u_2, \cdots, u_N\right\} \end{cases} \quad (3)$$

where $y(x)$ is the buckling load or the CFRP failure load , $p(x_i)$ is the basis function of the second order, $w(r_i)$ is a weight function using the fourth order spline function and r_i is the distance between the evaluation point and the calculation points defined in the D-optimal. The influence radius ρ was selected as the maximum norm (distance) between the evaluation point and the calculated 20 (in the case of buckling load) or 30 (in the case of CFRP failure load) points. When the accuracy of approximated results calculated from Equation (2) was examined for randomly selected 500 points in the space of design parameters, the average errors were 3.75 % for the buckling load and 4.62% for the failure load between both loads calculated directly from the FEM.

5.2 Optimum Calculation

The genetic algorithm (GA) method was used as an optimum algorithm here. In the genetic algorithm, the number of individuals, the values of crossover probability and mutation probability were 50, 0.5 and 0.03, respectively and the algorithm of the optimum search in GA was composed of four stages. In the first stage, the individuals having the design parameters were selected randomly and the object values according to the design parameters were calculated. When the buckling and failure loads obtained by the approximate functions,

respectively with the selected design parameters were smaller than the prescribed loads, these design parameters were not used and were changed to other parameters satisfying the constrain conditions.

The second stage is the selection of 50 individuals by using the roulette wheel method. The individual having the lowest weight among the 50 individuals was selected as the best individuals at the present generation. The best individual always remained at the next generation. This operation is called an elite preservation strategy and contributes to keeping the diversification and avoiding the initial convergence in the algorithm. 49 individuals were chosen with the roulette wheel method after the best individual in the second stage.

Two individuals were selected randomly in the third stage and this ratio of selection was called the crossover probability. Using the selected two individuals, some gene codes of one individual were swapped for the other gene codes. This operation meant to make other design variables. The final stage was mutation. Only one gene in the individual randomly selected from the 49 individuals in the third stage was changed to the other value of code depending on the mutation probability. This operation was useful to avoid a local minimum. The new individuals generated by the operations of the crossover and the mutation should be also examined to satisfy the constrain conditions. If the buckling and the failure loads were smaller than the prescribed loads, these individuals were rejected and other individuals were selected.

After the third stage was over, the GA calculation proceeded to one generation and there were usually some convergence conditions in the GA calculation. However, our GA calculation did not show any convergence criterion and was continued until the 300-th generations. Figure 4 shows the flow chart of the optimization.

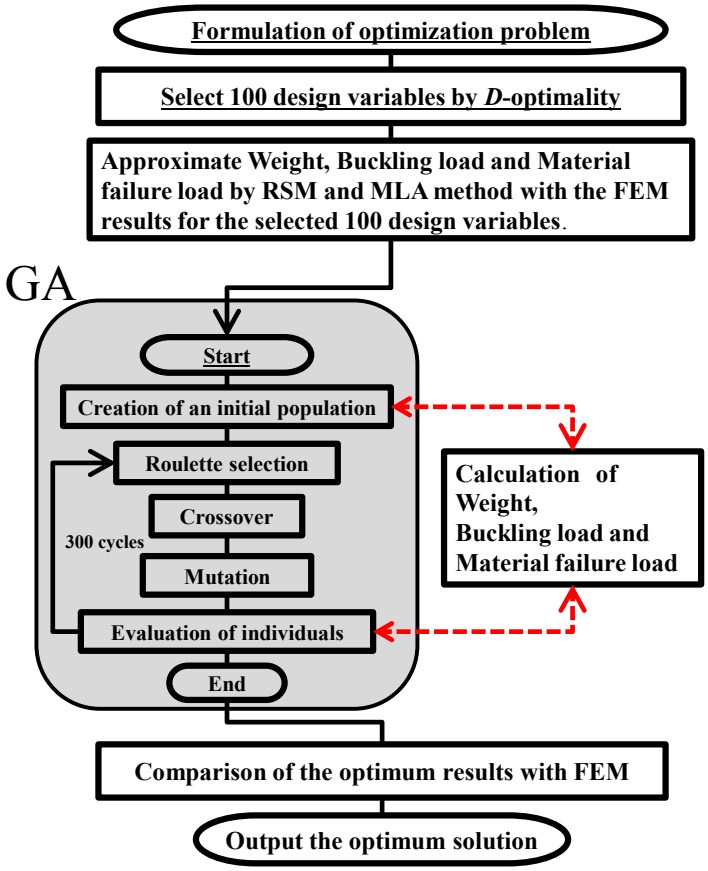

Figure 4 Flow chart of Optimization

5.3 Optimum results

Figures 5 and 6 show the changes of design parameters x1(winding angle) and x3(stacking layer numbers) against the generation during the iteration process of the GA calculation. The design parameter, x1, became a constant value for the three prescribed loads after 100 generations and the x3 became a constant value after 150 generations. The design parameter x2 also showed the same behavior as x3.

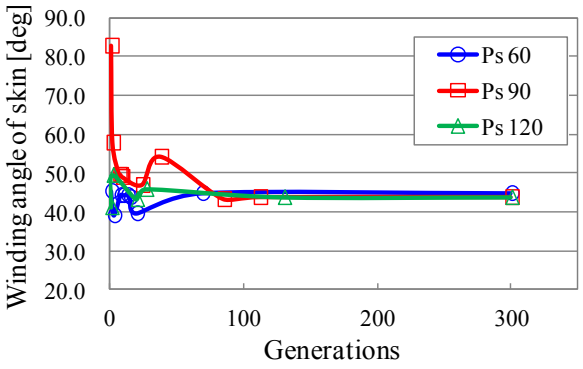

Figure 5 Relation of parameter x1 to generation

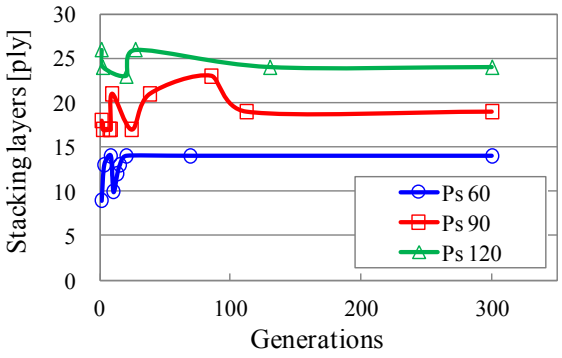

Figure 6 Relation of parameter x2 to generation

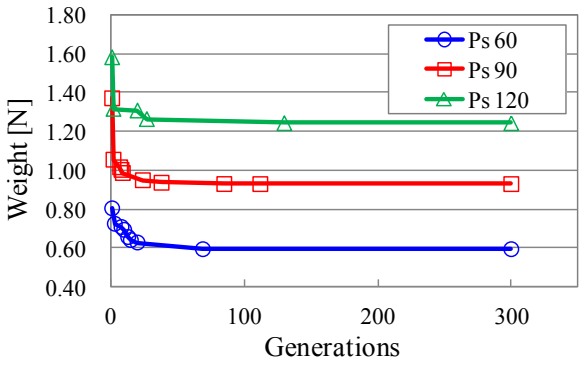

Figure 7 Relation of weight to generation

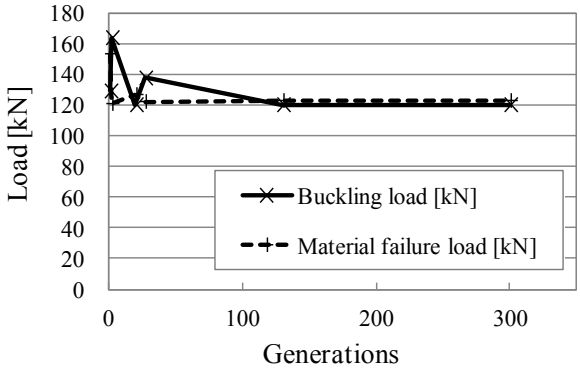

Figure 8 Relation of buckling load to generation

In Figure 7, the variation of the object function, W, is plotted against the generation for the three cases of prescribed loads of 60, 90 and 120 kN. The object function converged in less than 100 generations but the buckling load converged after 150 times of generation in the case of prescribed load of 120 kN as shown in Figure 8. As a result, the 150th generation time was enough in the calculation of GA for the optimum problem developed here.

In Table 6, the optimum design parameters and the resulting weights of CFRP isogrid shell under the prescribed loads of 60, 90 and 120 kN with the conditions of no buckling and no material failure are listed. By using the optimum design parameters obtained by the GA, the buckling load and the material failure load were calculated by the FEM and both results favorably agreed with each other. Furthermore, the prescribed loads of three cases were smaller than the corresponding buckling load and the material failure loads.

6. CONCLUSIONS

The axial compression tests and the linear and the nonlinear numerical calculations were carried out for the CFRP isogrid cylindrical shells and their optimum design method was examined. The following conclusions were drawn through this study:

(1) The maximum experimental compressive load of CFRP isogrid cylindrical shell was

higher than the sum of the maximum compression load of the two shells (a non-stiffened shell and a shell of grid alone). This fact showed the effect of reinforcements of CFRP cylindrical shells with the isogrid stiffeners.

(2) The axial compression tests of CFRP isogrid cylindrical shell with the surface skin winding angle of 90° showed the material failure and this was verified with the nonlinear FEM analysis and the Tsai-Wu criterion. On the other hand, the CFRP isogrid shell with the surface skin of a winding angle of 60° showed the buckling failure and this was also verified with the nonlinear FEM calculation.

(3) The experimental nonlinear behaviors of both CFRP isogrid cylindrical shells presented a good agreement with those calculated by the FEM.

(4) In the optimum design method of isogrid CFRP cylindrical shells, the width, the number of stacking layers (thickness) in the isogrid stiffeners and the winding angles of skin shell were selected as the design parameters and the weight of shell was set as the object function. This optimum problem was subjected to the constraint conditions of no bucking and no material failure under the uniaxial compression of three prescribed loads. The appropriate optimized numerical results were demonstrated here.

In this paper, the effect of delamination between the surface skin and the grid stiffeners was not investigated. In order to obtain closer agreement and the actual strength of CFRP isogrid cylindrical shell, the delamination in FEM analysis will be examined as the future work

	Optimum solution				GA (approximated values)		FEM	
Prescribed load [kN]	Weight [N]	x_1 Winding angle [deg]	x_2 Width [mm]	x_3 Stacking layers [ply]	Buckling load [kN]	Material Failure Load [kN]	Buckling load [kN]	Material Failure Load [kN]
60.0	0.595	44.9	2.06	14	61.2	68.2	62.1	63.7
90.0	0.928	43.8	2.83	19	90.8	98.1	91.1	95.9
120	1.25	43.8	3.27	24	120	123	121	125

Table 6 Optimization Results of design parameters and object value of weight

References

[1] T. D. Kim, Composite Structure,49, pp.21-25 (2000).

[2] G. Ben and N. Kishitani, Proceedings of the 6th Korea –Japan Joint Symposium on Composite Materials, p.156-157 (2007).

[3] A.D.Reddy, R.R.Valisetty and L.W.Rehfield, Continuous filament wound composite concepts for aircraft fuselage structures, Journal of Aircraft 22, pp.249-255 (1985).

[4] N.Jaunky, N,F,Knight and D.R.Ambur, Optimal design of grid- stiffened composite panels using global and local buckling analyses, Journal of Aircraft, 35(3), pp.478-486 (1998).

[5] N.Jaunky, N.F.Knight and D.R.Ambur, Optimal design of general stiffened composite circular cylinders for global buckling with strength constraints, Composite structures, 41, pp.243-252 (1998).

[6] D.R.Ambur and N.Jaunky, Optimal design of grid-stiffened panels and shells with variable curvature, Composite Structures, 52,pp.173-180 (2001).

[7] G.Totaro and Z.Gurdal, Optimal design of composite lattice shell structures for aerospace applications, Aerospace Science and Technology, 13, pp.157-164 (2009).